Failure Prediction for Polymer Products with Short Fiber

Junichi Takahashi[1], Yuki Fujita[1]

[1]ASAHI-KASE Corporation
1-3-2, Yakoh, Kawasaki-ku, Kawasaki-city, Kanagawa, 210-0863, Japan

1 Introduction

Polymers have been often used as structural materials under mechanically severe conditions instead of metals. We usually use FEM simulation when we design polymer products. The failure prediction of impact is especially important because its effect for reduction of development duration and number of trial products cannot be disregarded. The failure prediction has been investigated for a long time [1][2]. We generally start impact simulations using elasto-plastic material such as MAT_024 by giving stress-strain curves with strain rate dependency. We often add our own research achievement about material model by the user defined material models which LS-DYNA offers us to improve prediction accuracy.
We developed the isotropic material model based on damage of polymers and introduced it into LS-DYNA by using user subroutine "*MAT_041-050". We found many good coincidences between experimental impact test and numerical results with our material model. After that, we found the reason why we got good coincidence by simulation with isotropic material model was that glass fibers in the structural specimen of these experimental tests align well at the impact area.
Therefore, we decided to start simulations for structural specimens with various fiber distributions. Differences between the isotropic simulation results and anisotropic results are recognized. The importance for taking fiber orientation into account in impact simulations is known [3]. Then, we conducted the experimental impact tests using structural specimen made of Polyamide 66 with 35 weight% short fiber (ASAHI-KASEI Leona™ 14G35). We set different fiber distribution by giving two gate types in injection molding. In this paper, the effect of introducing fiber distribution is discussed.

2 Material tests

We focus on Polyamide 66 (ASAHI-KASEI Leona™ 14G35) under dry condition. We conducted high speed tensile tests using the testing machine controlled by servo hydraulic operation (Fig.1) to get stress-strain curves with strain rate dependency. Tensile speeds were set as 1mm/s, 10mm/s, 100mm/s, 1m/s and 10m/s. Tensile specimen with the geometry based on ISO 37 was made by injection molding. We set 30mm as the original distance L_0 that is the initial distance of grips in the direction of longitudinal axis. The lower grips are fixed. An imposed velocity is given to the upper grips. The imposed velocity U was given as 1mm/s, 10mm/s, 100mm/s, 1m/s and 10mm/s. If strain rates can be roughly estimated by U/L_0, each grip velocity corresponds to strain rates 0.033 s^{-1}, 0.33 s^{-1}, 3.3 s^{-1}, 33 s^{-1} and 330 s^{-1}, respectively. We obtained the load – displacement curves as shown in Fig.2.

Fig.1: Testing machine

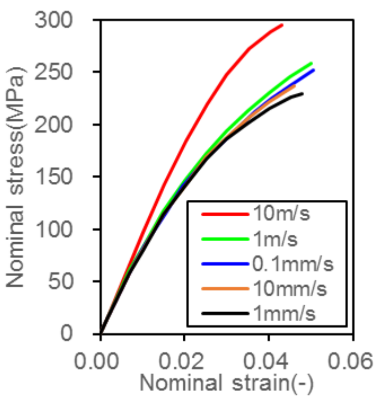

Fig.2: Tensile test Results

Fig.3: Drop tower Testing machine

3 Experimental impact tests

We conducted drop tower tests. Fracture processes were captured by high speed camera with 5000 frame/second as shown in Fig,3. A structural specimen with the geometry as shown in Fig.4 was fixed by jig as shown in Fig.5 and was plunged by the impactor with sphere top of 10mm radius and weight 10 kg. We used two types of structural specimen. The one was molded by single gate and the other was molded by double gates. The former has the top panel which fiber orientation relatively aligns well. The latter has the top panel which does not align at the vast area. We obtained the load-displacement diagram as shown in Fig.6 when we gave 1.3m/s as the impact speed.

4 Isotropic impact simulations

In this section we show two impact simulations using isotropic materials.

4.1 Simulation with elasto-plastic material model(MAT_024)

We could directly start an impact simulation if we had gauge length at narrow area and got true stress-true strain curves. However, we could not have gauge length when we use our high speed tensile test machine. So, we conducted tensile simulations at first to get true stress - true strain curves with strain rate dependency.
Next, we conducted impact test simulation for structural specimen using FE model as shown in Fig. 7. We predict fracture of structural specimen as shown in Fig.8. Then, we obtained the load–displacement relationship as shown in Fig.9. Experimental test result in case of single gate is also shown in Fig.9 as black line to compare it with the simulation result. The gradient of load-displacement relationship seems to be acceptable. And we can see the difference between the numerical displacement at breakage and the experimental one. We think so many countermeasures to cope with this difference although we did not try it in this study.
On the other hand, Fiber distribution in the top plate of structural specimen made by double gates is

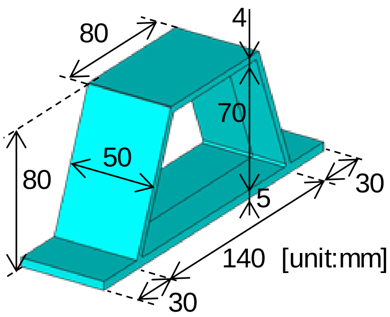

Fig.4: Structual specimen

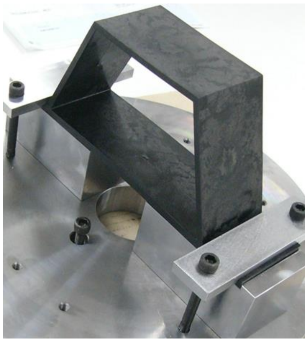

Fig.5: Fixing jig with specimen

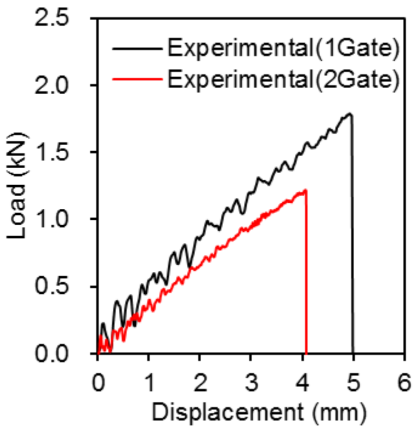

Fig.6: Impact test results

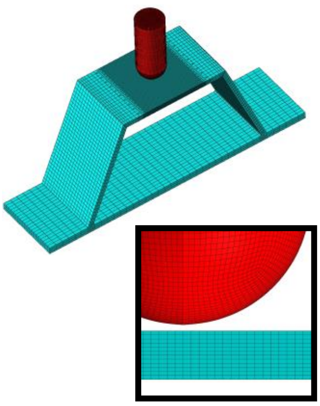

Fig.7: FE of structual specimen

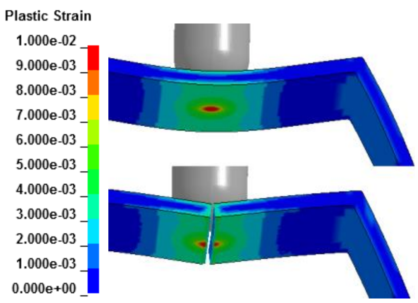

Fig.8: Fracture prediction

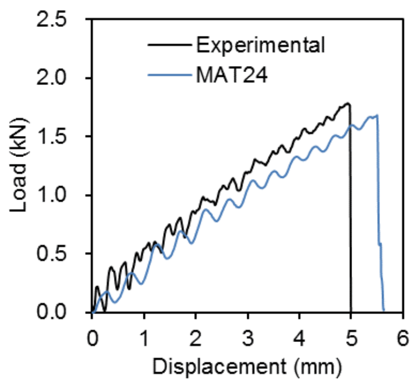

Fig.9: Load-displacement diagram of impact test with MAT024

too different from fiber distribution in the tensile specimen by injection molding. So, we can point out that we cannot compare this simulation result with the experimental test in case of double gates molding.

4.2 Simulation with Asahi-Kasei's material model with micro damage

We suggested a non-coaxial constitutive equation with craze effect [4] as

$$\overset{\nabla}{\boldsymbol{T}} = \boldsymbol{C}^v : \boldsymbol{D} - \dot{\bar{\varepsilon}}^p (\cos\delta) \boldsymbol{P}' - \frac{\dot{\omega}}{1-\omega} \boldsymbol{T} \quad (1)$$

$$\left.\begin{aligned} \boldsymbol{C}^v &\equiv \frac{H_\omega(1-\omega)}{H_\omega + 3\mu}\left[\boldsymbol{C}^e + \frac{3\mu}{H_\omega}\left\{\frac{3\lambda+2\mu}{3}\boldsymbol{I}\otimes\boldsymbol{I} + 3\mu\frac{\boldsymbol{T}'\otimes\boldsymbol{T}'}{\bar{\sigma}^2}\right\}\right] \\ \boldsymbol{P}' &\equiv \boldsymbol{C}^v : \boldsymbol{m}' = 3\mu(1-\omega)\frac{\boldsymbol{T}'}{\bar{\sigma}}, \qquad \boldsymbol{m}' \equiv \frac{3}{2}\frac{\boldsymbol{T}'}{\bar{\sigma}} \\ H_w &\equiv \frac{1}{(1-\omega)}\frac{\dot{\bar{\sigma}}}{\dot{\bar{\varepsilon}}^p k}, \qquad \dot{\bar{\sigma}} \equiv \sqrt{\frac{3}{2}\overset{\nabla}{\boldsymbol{T}}'\cdot\overset{\nabla}{\boldsymbol{T}}'} \end{aligned}\right\} \quad (2)$$

where, $\overset{\nabla}{\boldsymbol{T}}$ denotes the co-rotational rate of Cauchy stress $\boldsymbol{T}$, $\boldsymbol{D}$ the total deformation, $\dot{\bar{\varepsilon}}^p$ the equivalent plastic strain rate, δ the non-coaxial angle, μ and λ the Lamé constants, $\boldsymbol{T}'$ the deviatoric stress, σ the equivalent stress and k the non-coaxial parameter. As the hardening law, we use relations as

$$\dot{\bar{\varepsilon}}^p = \dot{\varepsilon}_r \left(\bar{\sigma}/g(\bar{\varepsilon}^p)\right)^{1/m} \quad (3)$$

$$g(\bar{\varepsilon}^p) = \sigma_r\left\{\tanh(k_1\bar{\varepsilon}^p) + k_2 + H_e(\bar{\varepsilon}^p - \varepsilon_h)k_3(\exp\bar{\varepsilon}^p - \exp\varepsilon_h) + k_4\bar{\varepsilon}^p\right\} \quad (4)$$

where, $\dot{\varepsilon}_r$ is the reference strain rate, g the flow stress, m the strain rate sensitivity, $\sigma_r k_2(\dot{\bar{\varepsilon}}^p/\dot{\varepsilon}_r)^m \equiv \sigma_y$ the initial yield stress in the case $\dot{\bar{\varepsilon}}^p = \dot{\varepsilon}_r$, ε_h the strain at which a rehardening begins and $H_e()$ the unit step function. In Eq. (4), k_1, k_2, k_3 and k_4 are non-dimensional material constants. We proposed an evolution equation of craze that is generally known as the damage peculiar to polymers as

$$\dot{\omega} = Af(\bar{\varepsilon}^p, \dot{\bar{\varepsilon}}^p)\dot{\bar{\varepsilon}}^p + B(1-\hat{\omega})\langle \dot{\varepsilon}_m^p \rangle \quad (5)$$

$$\left.\begin{aligned} f(\bar{\varepsilon}^p, \dot{\bar{\varepsilon}}^p) &= f_1(\dot{\bar{\varepsilon}}^p) f_2(\bar{\varepsilon}^p) \\ f_1(\dot{\bar{\varepsilon}}^p) &= \frac{1}{2}\left[1 + \tanh\left\{-D_1\left(\ln(\dot{\bar{\varepsilon}}^p/\dot{\varepsilon}_r) + D_2\right)\right\}\right] \\ f_2(\bar{\varepsilon}^p) &= \frac{1}{2}[1 + \tanh\{-D_3(\bar{\varepsilon}^p - \varepsilon_c)\}] \end{aligned}\right\} \quad (6)$$

where A, B, D_1, D_2 and D_3 are non-dimensional material constants and $\dot{\varepsilon}_m^p$ is the mean normal plastic strain. Then, ε_c denotes the strain at the beginning of growth cessation of craze.
Material constants of the above material model were closely examined. We programed Eq.(1)-(6) as usersubroutine and linked its object file with LS-DYNA solver. Using FE model as shown in Fig.8 we conducted the impact simulation with our material model. Then, we obtained Load– displacement diagram as the green curve in Fig.10. Comparing it with the black curve of the experimental result of

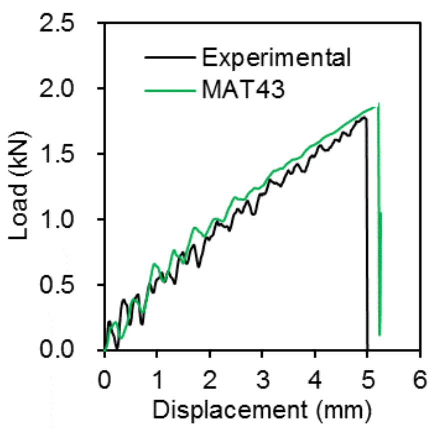

Fig.10: Load-displacement diagram of impact test by our material model

single gate molding we can see good coincidence for the gradient of load-displacement relationship and displacement at breakage. Concerning this good coincidence, we can point out that the fiber distribution on the top panel of structural specimen molded by single gate is close to the one on the narrow area of tensile specimen. However, we cannot compare this simulation result with the experimental double gates molding result because various fiber distribution is not taken into account in this simulation. This subject is left behind just same as the simulation by MAT024.

5 Anisotropic impact simulation based on fiber distribution

To resolve the subject mentioned above we decided to start anisotropic FE analysis based on fiber distribution. Nowadays, this analysis can be easily executed by using software “Digimat”.

5.1 Material properties based on fiber orientation

We cut out rectangular sheets for four different angles (0-degree, 20-degree, 45-degree and 90-degree) relative to flow direction from an injection molded plate (Fig.11). Tensile specimen with geometries based on ISO8256 TYPE3 is finally manufactured by milling. Tensile test results were gathered as shown in Fig.12. Identification to the material constants of Digimat is executed by optimization tool in Digimat-MX. Then, we got stress-strain curves for four different angles for Digimat as shown in Fig.13. We chose “Tsai-Hill 3D transversely isotropic by strain” as failure indicator. We are now testing at various tensile speeds to obtain the material properties with strain rate dependency. But, we cannot complete an identification. So, in this paper we use material properties based on quasi-static tensile test results although material constants with strain rate dependency should be used.

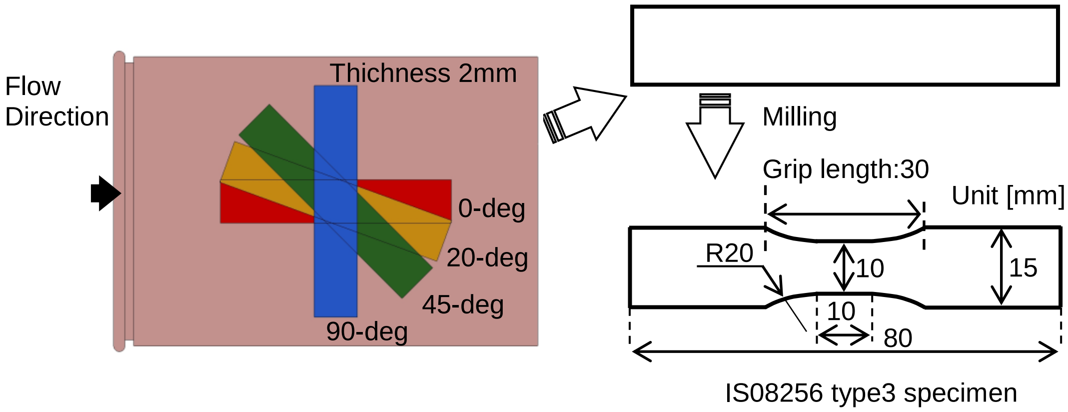

Fig.11 Specimens with various direction from an injection molded plate

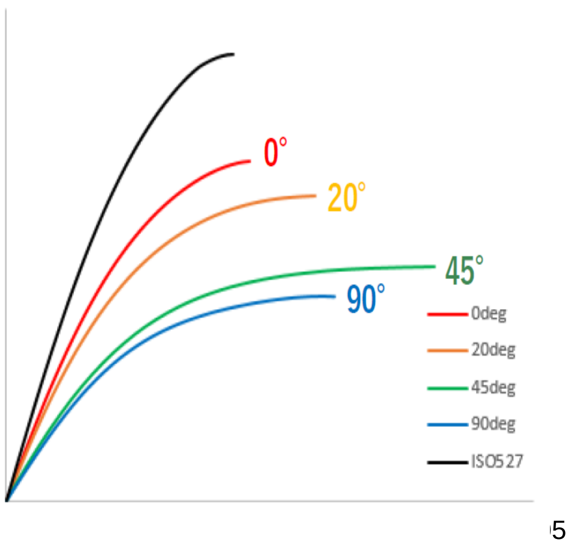

Fig.12: Experimental stress-strain curves

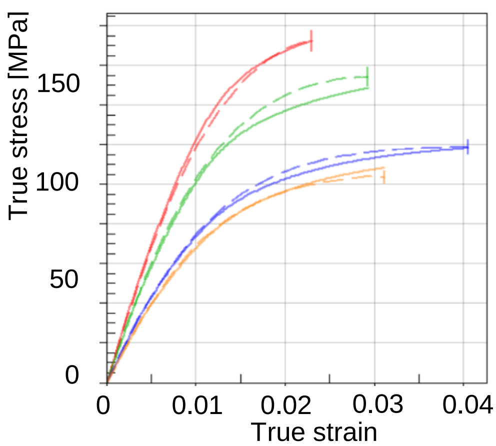

Fig.13: Identified curves for Digimat

5.2 Numerical prediction of fiber orientation in structural specimen

Injection molding simulation is generally conducted to obtain distribution of fiber orientation of structural specimen. Results by molding software "MOLDFLOW" are shown in Fig.14. Fiber orientation in the top plate aligns well in case of single gate because fiber orientation tensor is relatively colored red. On the other hand, we can see weld lines in the top plate and the bottom plate in case of double gates. And we can say that fiber orientation in the top plate in case is more random than the one of single gate because fiber orientation tensor is colored yellow in vast area of the top plate. Distribution data of fiber orientation calculated by injection molding software are mapped by Digimat-MAP to elements of LS-DYNA as shown in Fig.15.

5.3 Impact simulation by LS-DYNA with Digimat

Load-displacement curve colored light blue in Fig.16 is the numerical result of structural specimen molded by single gate. Concerning the gradient of load-displacement relationship we can see good correspondence between the light blue curve and the black curve of the experimental result. However, numerical breakage begins at the displacement 3mm which is 2mm smaller than the experimental breakage. The magenta curve in Fig.16 is the numerical result of the structural specimen molded by double gates. We show the light blue line i.e. single gate molding specimen's result again to compare the difference between single and double gate molding. We can say that the difference is so small than the experimental difference as shown in Fig.6.

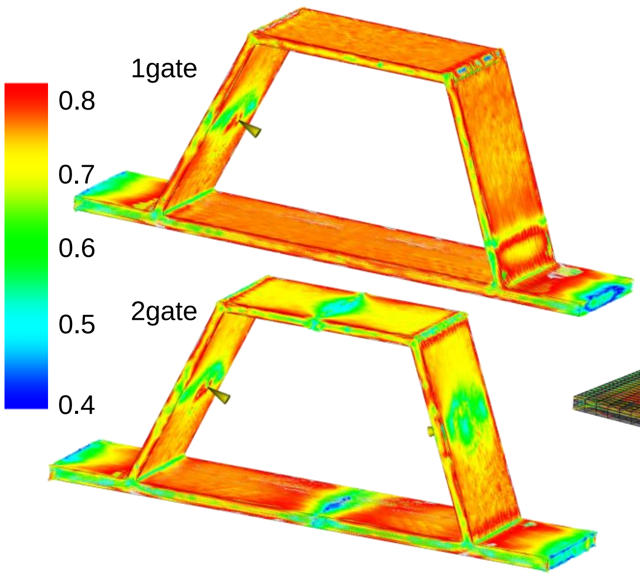

Fig.14: Vector polt of fiber orientation

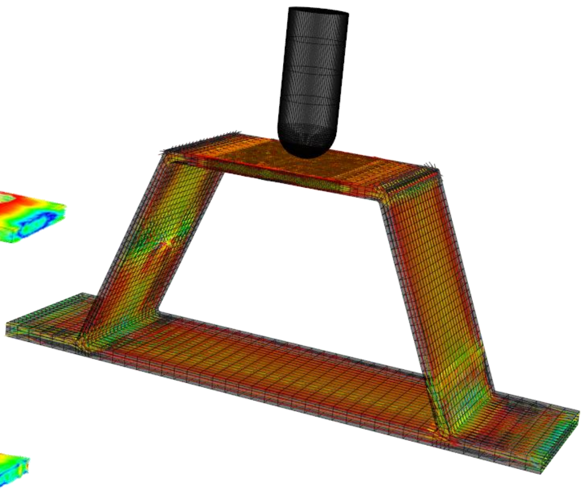

Fig.15: Stractural FE with fiber orientation

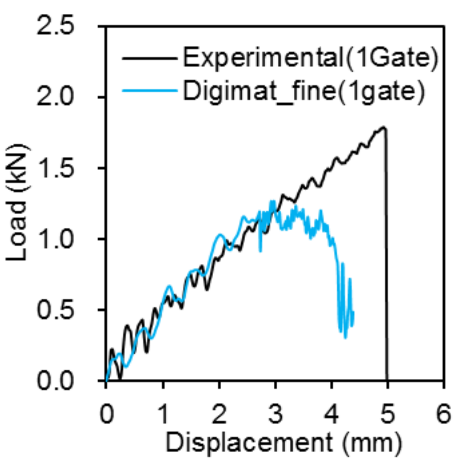

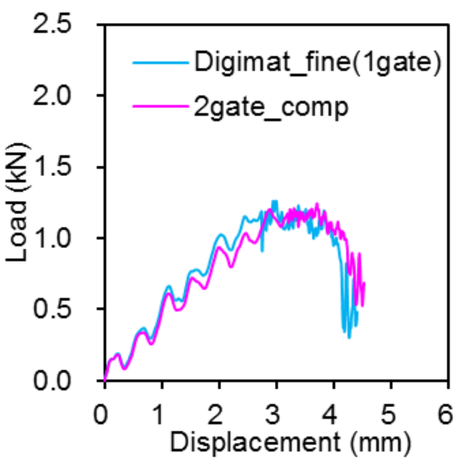

Fig.16: Load-displacement diagram of impact test by our material model

Summary of simulations mentioned above is shown in table.1. The gradient of load-displacement relationship in case of simulation with single gate molding can be acceptable even though an isotropic material model is used. In this study the numerical result by our material model shows good coincidence with the experimental displacement at breakage. Then, numerical result by MAT024 will improve the coincidence with the experimental result if we try to identify material constants more closely or use an additional function *MAT_ADD. Useful simulation for double gate molding may be conducted if we can conduct tensile tests with the tensile specimen which has same fiber distribution as a structural specimen molded by double gates. But it is not realistic because fiber distribution on the top plate of structural specimen must be terribly various. So, we can say that an isotropic material cannot be applied to the structural specimen by double gates.
In this point of view, Digimat is the strong tool. An accurate distribution of fiber orientation tensor should be predicted by molding simulation software. An accuracy of numerical fiber distribution can be quantified by comparing it with the experimental observation of real structural specimen. So, we expected the effect of introducing distribution of fiber orientation by Digimat. But, now we find necessity to find suitable FE modeling for introducing fiber distribution or find suitable failure indicator for our material. Optional parameters i.e. damage or stress triaxiality dependency may be needed for improving a numerical breakage. Now many subjects are left behind but we will overcome these subjects because user defined failure indicator can be used just same as the user defined material model in LS-DYNA.

Table 1: Summary of simulations in this study

	Single gate molding specimen		*Double gates molding specimen*	
	Load-disp. gradient	*Breakage disp.*	*Load-disp. gradient*	*Breakage disp.*
MAT024	*Better*	*Better*	*Can not predict*	
User-defined	*Good*	*Good*		
Digimat	*Good*	*No Good*	*Better*	*No Good*

6 Summary

Impact simulations using MAT024, the user defined material model and Digimat are conducted. We summarize as below.

1. Impact simulation with Isotropic material model such as MAT024 can be applied to the structural specimen which has same fiber distribution as tensile specimen. Using user defined material model MAT041-050, we can easily develop own isotropic material model for own polymer material to improve load-displacement relationship in impact simulation.
2. Subject to be solved in the impact simulation using isotropic material model mentioned above is that these material model cannot deal with the structural specimen which has terribly different distribution of fiber orientation to the tensile specimen.
3. We confirm that Digimat brings the different load-displacement curve in impact simulation when we calculate impact test using the specimens with different fiber distribution. Actually, Digimat is the strong tool which can dell well with various fiber distribution. But, we find that a fracture prediction in Digimat should be revised. We will apply our experiences in developing an isotropic material model using LS-DYNA's user defined material to fracture criterion in Digimat.

7 Literature

References should be given in the last paragraph of your manuscript. Please use following scheme:

[1] H. Diyan, F. Grytten, E. Andreassen, H. Osnes, R.H. Gaarder, E.L. Hinrichsen: "Numerical simulation of low-velocity impact loading of polymeric materials", 7th European LS-DYNA Conference, Salzburg, 2009.
[2] S. Hayashi: "Prediction of Failure Behaviors in Polymers Under Multiaxial Stress State", 12th International LS-DYNA Users Conference, Detroit, 2012.
[3] T. Sakakibara, R. Akita, Y. Ohnishi, S. Kigima, Y. Kanki, M. Seto, K.Suda, K. Yamakawa and Y. Ayano: "Simulation of all impact on composite plate with PP+30% LGF", 12th International LS-DYNA Users Conference, Detroit, 2012.
[4] J. Takahashi, T. Yamamoto, and K. Shizawa, "Modeling and Simulation for Ductile Fracture Prediction of Crystalline Polymer Based on Craze Behavior", International Journal of Mechanical Sciences, Vol. 52-2, (2010), pp.266-276.